IL NUOVO CIMENTO VOL. 20 C, N. 3 Maggio-Giugno 1997

Reliability of third-order moment parameterization for models of turbulent boundary layer over gentle topography(*)(**)

A. MAURIZI, F. TROMBETTI, S. DI SABATINO and F. TAMPIERI

Istituto FISBAT-CNR - Via Gobetti 101, I-40129 Bologna, Italy

(ricevuto il 10 Gennaio 1996; approvato il 23 Settembre 1996)

Summary. — An analysis is made of the transport equation of Reynolds shear stress, written in a streamline coordinate system, starting from the fields of first- and second-order moments of wind velocity, measured in a terrain-following system over gentle topography, in order to verify the usual parameterizations of third-order moments. The equation is split into two parts: the first contains the terms which can be calculated directly from measurements, the second involves the pressure-velocity correlation considering the terms of rapid distortion, curvature and return to isotropy and the transport of triple velocity-correlation modelled assuming a flux-gradient approximation. Moreover, the error estimates associated with both parts have been computed using a Monte Carlo technique which takes into account the experimental errors. This analysis is performed on wind tunnel data over a gently shaped two-dimensional valley and hill. The comparison between the measured and modelled parts is good near the surface, whereas, at higher levels, where the pertubations induced by the topography are significant, there are large zones generally characterized by streamlines with concave curvature in which the flux-gradient approximation used to compute the triple product correlation cannot be applied.

PACS 92.60.Fm – Boundary layer structure and processes.
PACS 92.60.Ek – Convection, turbulence and diffusion.
PACS 92.60 – Meteorology.
PACS 92.10.Lq – Turbulence and diffusion.
PACS 01.30.Cc – Conference proceedings.

1. – Introduction

Understanding and modelling the influence of topography on turbulent flow is of great importance in many practical applications, such as the transport and deposition of

(*) Paper presented at EUROMECH Colloquium 338 "Atmospheric Turbulence and Dispersion in Complex Terrain" and ERCOFTAC Workshop "Data on Turbulence and Dispersion in Complex Atmospheric Flows", Bologna, 4-7 September 1995.
(**) The authors of this paper have agreed to not receive the proofs for correction.

pollutants, wild-fire prevention, wind energy supply, etc., and is necessary for the boundary layer parameterization in general circulation models. Numerical or analytical models based on first- (mixing-length or eddy diffusivity) or one-and-a-half order (E-ϵ) closure for Reynolds stresses allow the mean wind field to be predicted with good accuracy [1], whereas they fail to reproduce turbulence modifications also above gentle topography, as fully discussed in many recent works [2–5]. Therefore, to take into account the non-equilibrium effects induced by topography, it is necessary to use at least a second-order closure model [6] that still contains third-order moments, which are usually not measured and thus require an appropriate parameterization.

Field experiment data sets, even if highly accurate (as in the case of the Askervein Hill experiment, see [7]) give only a few vertical profiles of turbulence quantities, so that it is impossible to have sufficiently detailed information with horizontal and vertical resolution to validate turbulent boundary layer models. An alternative to field data is offered by wind tunnel experiments, which allow good measurement quality and a large number of vertical profiles of mean and turbulent variables in different positions with respect to the topography [8–13], even if limited to Reynolds number smaller than in the atmospheric boundary layer and often made in neutral conditions.

This work is based on the RUSHIL [8] and RUSVAL [10, 14] turbulence data set analysis. The flow fields in terrain-following coordinate system, reconstructed from the measured vertical profiles of first- and second-order moments of wind velocity components, are transformed into the streamline coordinate system (the most appropriate to study flow over topography) in order to evaluate the terms of Reynolds shear stress balance equation.

In our analysis we calculate separately the terms that can be obtained directly from measurement and those that have to be parameterized because they involve the non-measured third-order moments. Moreover, applying a Monte Carlo technique, which takes into account experimental errors of measurement, we compute the uncertainty associated with both parts of the balance equation.

A description of the data set is presented in sect. **2**. In sect. **3** we outline the method used to transform terrain-following data into a streamline coordinate system and write the Reynolds shear stress equation in this coordinate system. In sect. **4** the models adopted to evaluate pressure-strain redistribution and the turbulent-transport term are summarized together with the procedure for error analysis. In sect. **5** a comparison is made between the measured and modelled terms computed along different streamlines above a gently shaped hill and valley and some remarks are made about the proposed model performances. Finally, some conclusions are drawn in sect. **5**.

2. – Wind tunnel data set and its preliminary analysis description

The data sets consist of the wind data obtained from the US EPA wind tunnel experiments RUSHIL [8] and RUSVAL [10,14] on flow structure and tracer dispersion over isolated 2D hills and valleys. The wind tunnel simulates a neutral boundary layer of about 1 m height, characterized by a logarithmic wind profile with friction velocity $u_* = 0.19\,\mathrm{m\,s^{-1}}$, roughness length $z_0 = 1.6 \cdot 10^{-4}$ m, displacement height $d_0 = -2 \cdot 10^{-3}$ m and free stream velocity $U_\infty = 4\,\mathrm{m\,s^{-1}}$, leading to a Reynolds number of about $2 \cdot 10^5$. A 2D model hill or valley of analytical shape, symmetrical about the vertical axis z, is placed across the oncoming flow (x-direction), spanning the width of the tunnel (y-direction). Three models with a maximum height or depth $H = 0.117\,\mathrm{m}$ are used. Their aspect ratios (ratio of the half-width a to H) are 8, 5 and 3. All the models have the same roughness as

the wind tunnel floor. Vertical profiles of mean horizontal velocity U, flow angle α (angle of mean velocity with respect to horizontal surface), standard deviations of longitudinal ($\sigma_u = (\overline{u^2})^{1/2}$), vertical ($\sigma_w = (\overline{w^2})^{1/2}$), lateral ($\sigma_v = (\overline{v^2})^{1/2}$ only for V8) fluctuating velocity components and Reynolds shear stress $\overline{uw}$ are measured at 15 or 16 longitudinal locations from $x/a = -2$ to $x/a \simeq 5$, where $x = 0$ corresponds to the hill or valley centre and z is the height above topography. All the measurements are made with a hot-wire anemometer and, in the RUSVAL experiment also with a pulsed-wire anemometer where the turbulence intensities are very high ($> 20\%$) and even in reversing flow region. Each vertical profile is smoothed taking into account the errors of experimental measurements ($0.05\ \mathrm{m\,s^{-1}}$ for the mean wind velocity, 0.5 degrees for the flow angle and a relative error of about 10% for second-order moments) and is subsequently interpolated at 81 regularly spaced intervals in a vertical log-scale referring to the ground surface [15, 16].

3. – Coordinate systems and data treatment

3˙1. *Terrain-following coordinate system.* – The available data implicitly define a terrain-following coordinate system as

$$\left\{ \begin{array}{lcl} \hat{x} & = & x\,, \\ \hat{z} & = & z - h(x)\,, \end{array} \right. \tag{1}$$

where $h(x)$ is the topography, $(\hat{x}, \hat{z})$ are the terrain-following coordinates and (x, z) are the Cartesian ones.

The domain is transformed by (1) into a rectangular grid, the "natural" one in which fitting and differentiation can easily be performed. In fact, the directional derivatives in the $(\hat{x}, \hat{z})$ space are exactly the incremental ratio limit for any function of these variables. Turbulence fields (Cartesian components of mean velocity vector and Reynolds stress tensor) are reconstructed in the $(\hat{x}, \hat{z})$ space, fitting data at constant $\hat{z}$. Differentiation is performed both at constant $\hat{x}$ and $\hat{z}$, by computing the derivatives of interpolating Akima cubic splines [17].

As regards the mean velocity, in order to satisfy the continuity equation for incompressible fluid, the field is reconstructed from the streamfunction ψ which, applying the no-slip conditions at the boundary in the terrain-following coordinate system, reads:

$$\psi(\hat{x}, \hat{z}) - \psi_0 = \int_{(\hat{x},0)}^{(\hat{x},\hat{z})} \hat{U}(\hat{x}, \tau)\mathrm{d}\tau\,, \tag{2}$$

provided that the integration path for the $\hat{x}$ direction lies on the solid boundary. The mean velocity field, reconstructed in this way, shows good agreement with the present data set [18].

3˙2. *Streamline coordinate system.* – While the terrain-following coordinate system is the most appropriate in treating data, analysis of the equations in a streamline coordinate system allows us to emphasize the quantities involved with curvature, so that the streamline coordinate system is shown to be very useful in capturing the main features of a distorted flow. The streamline coordinate system is defined as

$$\left\{ \begin{array}{lcl} \xi & = & \phi(x, z)\,, \\ \zeta & = & \psi(x, z)\,, \end{array} \right. \tag{3}$$

where ψ is the streamfunction and ϕ is the pseudo-potential function which can be derived by imposing the perpendicularity condition between the ϕ- and ψ-curves.

After the transformation procedure outlined in [19], and assuming that viscous dissipation is negligible [20], the equation for Reynolds shear stress in this frame is

$$U\frac{\partial\,\overline{uw}}{\partial\xi}+\overline{w^2}\,\frac{\partial U}{\partial\zeta}-2\overline{u^2}\,\frac{U}{R}+\overline{w^2}\,\frac{U}{R}=-\Pi-\Theta\,, \tag{4}$$

where the left-hand side can be computed directly from data, while the right-hand side has to be modelled. In eq. (4), R is the local radius of curvature of the ψ coordinate lines, Θ represents the turbulent transport terms and Π the pressure-velocity correlation terms.

All variables in eq. (4) are intended to be "physical components", *i.e.* quantities that would be measured by an instrument aligned with a base vector [21]. For the sake of simplicity, we use ξ and ζ to indicate the physical components of the coordinates defined by eqs.(3). It should be observed that the derivatives in eq. (4) are directional rather than partial [11] and are computed from terrain-following directional derivatives following [18].

4. – Closure models and error analysis

4˙1. *Models.* – In order to close eq. (4), the following models for the Π and Θ terms have been adopted. The model for the Π term is the one proposed by [6], *i.e.*

$$\Pi=\Pi^d+\Pi^c+\Pi^r\,, \tag{5}$$

where

$$\Pi^d=-\frac{\partial U}{\partial\zeta}\sum_i\delta_i\overline{u_i^2} \tag{6}$$

is the contribution due to rapid distortion [22], in which $u_1=u$, $u_2=v$, $u_3=w$ and the three constants δ_i are to be determined from the data. The second term of eq. (5),

$$\Pi^c=2(\delta_3-\delta_1)(\overline{u^2}-\frac{1}{2}\overline{w^2})\frac{U}{R}, \tag{7}$$

is due to streamline curvature, and the third one,

$$\Pi^r=C\epsilon\frac{\overline{uw}}{q^2}, \tag{8}$$

is due to the return to isotropy [23], where ϵ is the average dissipation rate of turbulent kinetic energy $q^2/2=\sum_i\overline{u_i^2}$. The constants $\delta_1=0.12$, $\delta_3=0.56$, $\delta_2=\delta_1+\delta_3-1/5=0.48$ and $C=2.77$ have been evaluated following [22], taking into account that in the surface layer of the unperturbed boundary layer measured in the wind tunnel the values $\sigma_u/u_*=2.5$, $\sigma_w/u_*=1.3$, $\sigma_v/u_*=1.8$ and $q^2/u_*^2=11.2$ are observed.

It should be noted that the dissipation rate ϵ also needs to be modelled, but it enters into eq. (4) indirectly through eq. (8). It is assumed that the turbulence time scale T is unique, so we can write

$$\epsilon=\frac{q^2}{2T}\,, \tag{9}$$

where T can be estimated from a mixing-length model proposed by [24] which is particularly good to determine the vertical momentum flux with the present data set [5]. Thus

$$T = C_T \frac{\ell_z}{\sigma_w}\,, \tag{10}$$

where

$$\ell_z = \left(\frac{1}{\ell_0} + \frac{b}{z} + c\frac{|\partial_\zeta U|}{\sigma_w}\right)^{-1} \tag{11}$$

and $C_T = 0.137$ is determined by taking the surface layer relationships to be valid. The coefficients in eq. (11) are: $\ell_0 = 0.4$ m, $b = 0.58$ and $c = 1$.

Concerning the transport terms in eq. (4), a flux-gradient model is adopted [6, 25] to evaluate the triple velocity product. It is assumed that horizontal diffusion and curvature effects are negligible, and therefore only the vertical transport is considered significant. Thus,

$$\Theta = \frac{\partial \overline{uw^2}}{\partial\, \zeta} = \frac{\partial}{\partial \zeta}\left(-\nu_\Theta \frac{\partial\, \overline{uw}}{\partial \zeta}\right) \tag{12}$$

in which the eddy diffusion coefficient is evaluated as

$$\nu_\Theta = C_\nu \overline{w^2} \frac{q^2}{2\epsilon} = C_\nu C_T \sigma_w \ell_z\,, \tag{13}$$

where $C_\nu = 0.23$ is assumed from [26].

4·2. *Error analysis.* – The two sides of eq. (4) are treated as two distinct statistical ensembles, where each variable, *e.g.* G, is written in the form treat the two sides of eq. (4) as the mean values of two distinct statistical ensembles, where the variables $U, \overline{u^2}, \ldots$ are independent and affected by random errors.

$$G + \Delta_\gamma G\,, \tag{14}$$

where $\Delta_\gamma G$ is the absolute error associated with G, multiplied by a number extracted from a Gaussian distribution with zero mean and unit variance. zero mean and unitary variance. Thus, the left-hand side of eq. (4), *i.e.* the measured (Meas.) part, becomes:

$$\begin{aligned}\text{Meas.} \;=\; & (U + \Delta_\gamma U)\frac{\partial\, \overline{uw}}{\partial x}\left(1 + \frac{\Delta_\gamma \overline{uw}}{\overline{uw}}\right) + (\overline{w^2} + \Delta_\gamma \overline{w^2})\frac{\partial U}{\partial z}\left(1 + \frac{\Delta_\gamma U}{U}\right) - \\ & -2(\overline{u^2} + \Delta_\gamma \overline{u^2})\frac{U + \Delta_\gamma U}{R} + (\overline{w^2} + \Delta_\gamma \overline{w^2})\frac{U + \Delta_\gamma U}{R}\,,\end{aligned} \tag{15}$$

where we assumed that R is an exact value and errors in numerical differentiation are negligible and are thus assumed to be equal to errors associated with the corresponding undifferentiated quantities.

Taking the average of a sufficiently large number of realizations, the mean value of (15) is equal to the left-hand side of eq. (4), while standard deviation gives the desired error estimate associated with the whole measured part.

The same procedure is applied to the right-hand side of eq. (4) in order to evaluate the error band associated with the modelled part. In fact, since models are written in terms of variables affected by experimental errors, the results present an uncertainty depending on errors associated with measured quantities.

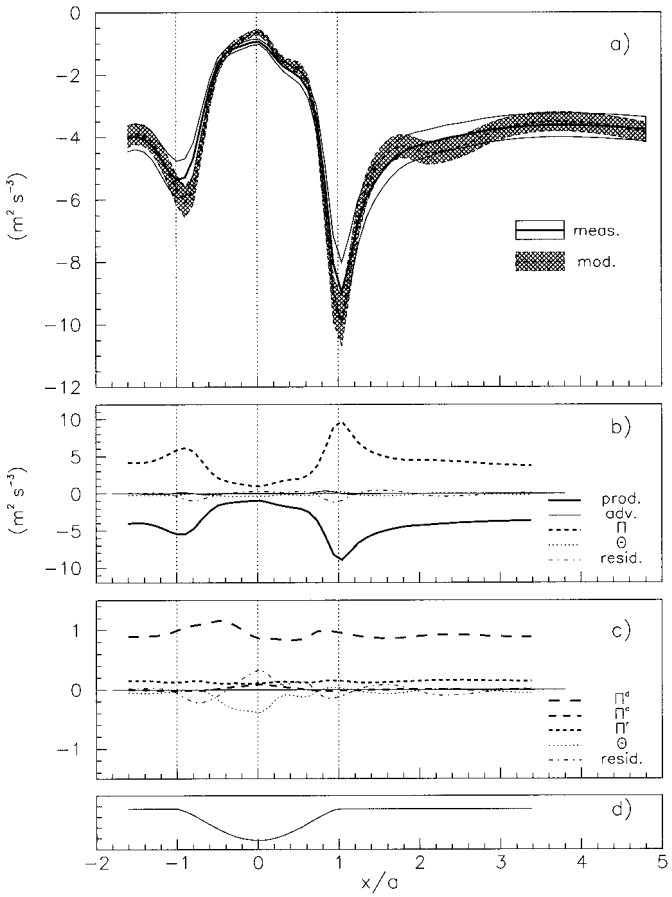

Fig. 1. – Comparison between measured and modelled parts of Reynolds shear stress balance (eq. (4)) along the streamline originating at $\hat{z}_{s-\infty} = H/20$ for the V8 case: a) mean results and associated error bands; b) terms of balance; c) ratios between single modelled terms and total measured part. The vertical dotted lines indicate the beginning, middle and end of the valley shown at the bottom d) (the vertical scale is magnified).

5. – Results and discussion

The method outlined in sect. **3** and fully described in [18] for the treatment of flow data measured over topography has been applied to the turbulence data set referring to the wind tunnel experiments over the 2D hill and valley with aspect ratio 8 (labelled H8 and V8, respectively) described in sect. **2**.

At first we reconstruct the mean velocity field to satisfy the continuity equation from the streamfunction. Then we derive the streamlines whose height above ground is given by

$$\hat{z}_s(\hat{x}, \psi_0) = \int_0^{\psi_0} \frac{\mathrm{d}\psi}{\hat{U}} \tag{16}$$

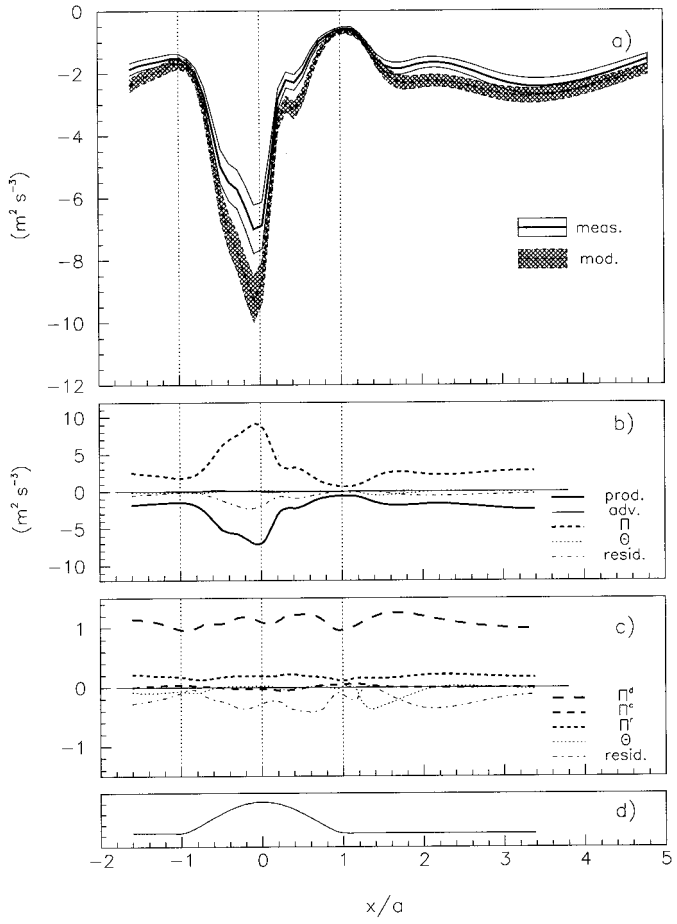

Fig. 2. – As in fig. 1, but for the H8 case.

and their curvature radius R [6] is

$$\frac{1}{R} = -\frac{\partial^2 z_s}{\partial x^2}\left[1 + \left(\frac{\partial z_s}{\partial x}\right)^2\right]^{-3/2}, \tag{17}$$

where $z_s = \hat{z}_s + h(x^1)$.

We compute all the terms of the transport equation of Reynolds shear stress (eq. (4)) along the streamlines, both those directly obtained from measurements (left side) and those modelled (right side) with their associated errors. As mentioned in sect. **2**, the measurements of $\overline{v^2}$ are available only for the V8 experiment. Thus, to compute q^2 (and then the rapid distortion and the return to isotropy terms of the pressure-strain redistribution) in the H8 experiment, we took, as the $\overline{v^2}$ field, the ones obtained from a linear interpolation between the first and last profile of the V8 experiment, since these profiles were not perturbed by the valley. Obviously, this assumption does not account for the perturbation induced by the hill, but it does give the proper order of magnitude of the turbulent kinetic energy. The comparison between the results obtained using the real data and the above assumption in the V8 experiment showed that the amount of error introduced in the terms

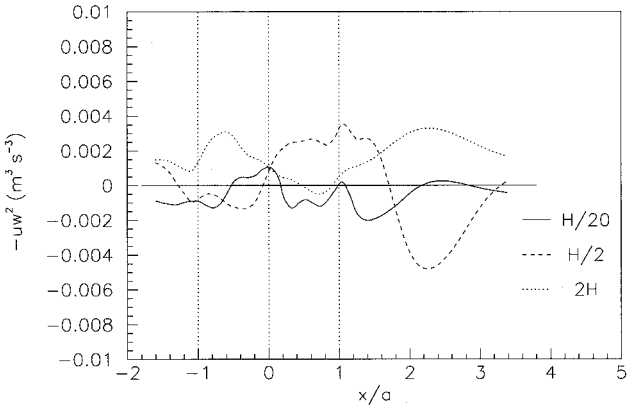

Fig. 3. – $-\overline{uw^2}$ computed from the flux-gradient approximation (eq. (12)) along the three selected streamlines over H8.

containing q^2 is minimal (see [27]).

To test the validity of the proposed models for pressure-velocity and turbulent transport terms in the different zones of the boundary layer perturbed by the hill and valley, we compare the model results with the measured ones along three different streamlines, whose heights $\hat{z}_{s-\infty}$ on the flat ground far upwind of the obstacles are: $H/20$ (*i.e.* about 6 mm, the lowermost measurement height), $H/2$ and $2H$.

At the lowest height for V8 (fig. 1a) the general agreement is quite good: the two curves with their respective error bands are superimposed over almost the entire domain, whereas for H8 (fig. 2a) the models overestimate in the convex region of the flow around the hill top. Looking at the details in the V8 experiment (fig. 1b), the total production is balanced by the pressure-velocity term Π, and mainly by its rapid distortion component (fig. 1c). In the case of H8 (fig. 2b), the pressure term is greater than the production in the convex zone and probably the rapid distortion term is overestimated, as can be inferred from the behaviour of the residual term (fig. 2c). The turbulent transport is relatively small in both cases: in the concave region of the flow upwind of the hill (approximately up to $-0.5\,x/a$) it is negative, as direct measurements made by [13] in the wind tunnel

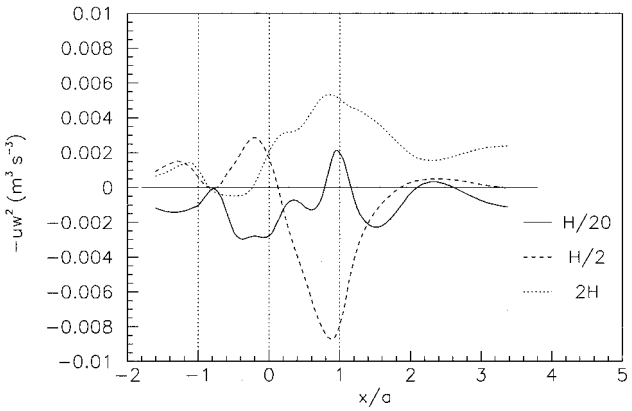

Fig. 4. – As in fig. 3, but for V8.

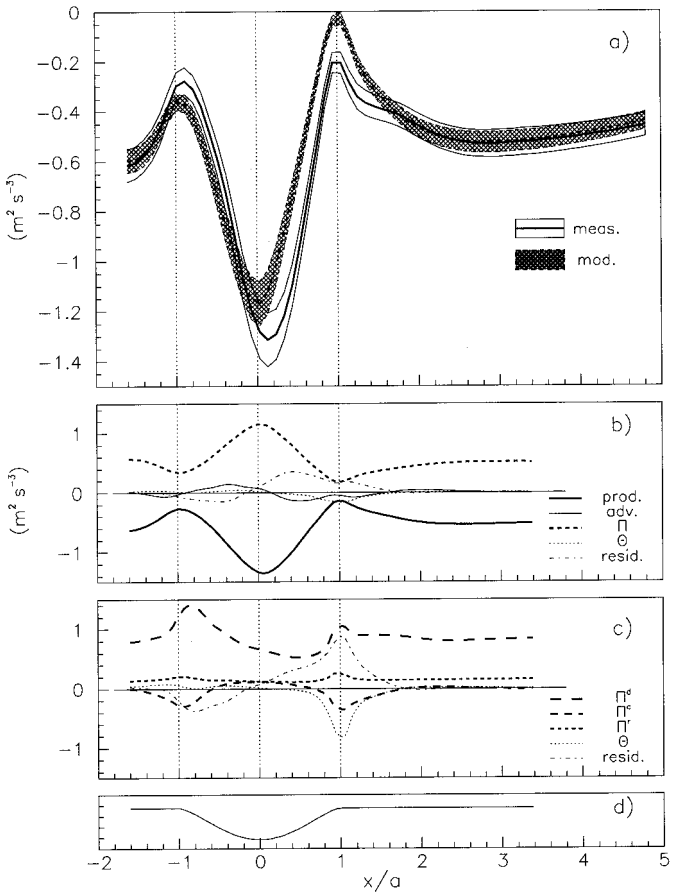

Fig. 5. – As in fig. 1, but for $\hat{z}_{s-\infty} = H/2$.

experiment above a steeper hill indicate (see, for example [13], the values near the wall of the profiles of this term at $x = 1015$ and 1183 mm in their figs. 6b and 7b). Moreover, their measured profiles of $-\overline{uw}$ at the same position ([13], fig. 2b) near the wall, show positive values of the vertical gradient, so that eq. (12) gives negative values of $-\overline{uw^2}$. The measured values of $-\overline{uw^2}$ (see again [13], fig. 3c) are themselves negative, confirming the validity of the flux-gradient assumption. Also in our case, at the lowest level $-\overline{uw^2}$ is negative (see fig. 3). In the convex region around the H8 top the estimated transport term is practically null and the computed $-\overline{uw^2}$ values are positive, according to the measurements of [13] (see their data at $x = 1345$, 1596, 1665 and 1862 mm). In the lee of H8, $-\overline{uw^2}$ again becomes negative according to the concave upwind region data, but these results are not directly comparable with experimental measurements because the Baskaran hill separates and the data in the lee region are not available. An analogous behaviour of $-\overline{uw^2}$ can be noted in V8 (fig. 4), *i.e.* negative values in the concave zone (from approximately -0.5 up to $0.5\, x/a$) and positive or null in the convex ones (around the edges of the valley). This result is consistent with the consideration that in the inner layer, whose depth, for the present experiments, turns out to be about 30 mm or 10 mm following [28] or [29] respectively, a flux-gradient diffusion approach for the triple velocity correlation may be assumed.

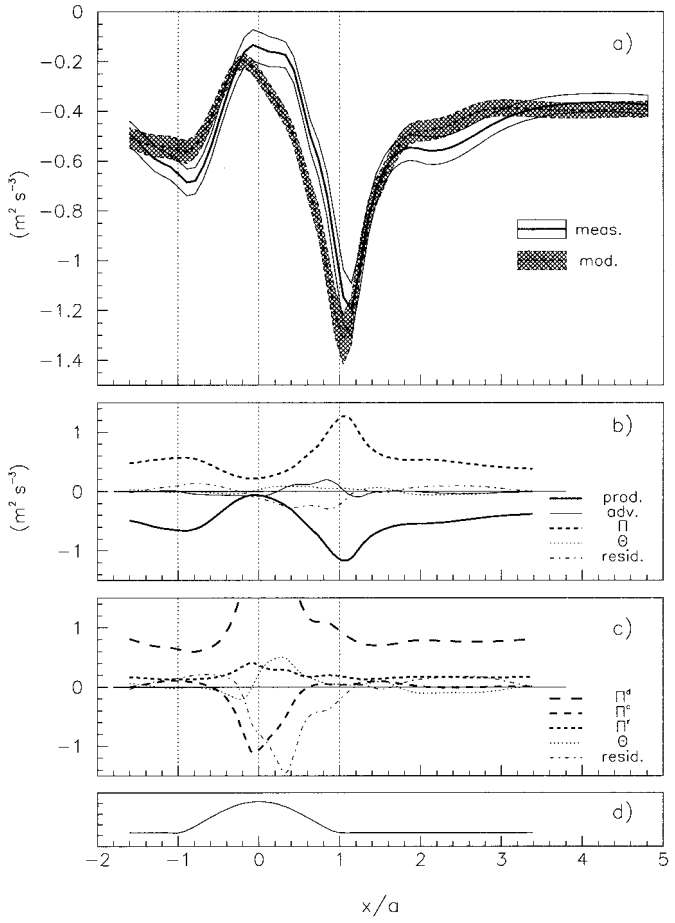

Fig. 6. – As in fig. 5, but for H8.

In the intermediate layers the model results are less accurate (figs. 5a and 6a). In fact, where the vertical profiles of $-\overline{uw}$ increase with height (see [15] and [16]), eq. (12) gives negative values of $-\overline{uw^2}$ (figs. 3 and 4) in contrast with the direct measurements of [13]. Therefore, the evaluation of the transport term is wrong in these zones, which, in V8, correspond to those where the residual term (which contains the model error) is greater (see fig. 5a). An example of the results obtained in this case, neglecting the transport term, is given in fig. 7, where a clear improvement can be observed around the exit of the valley. As far as the Π term is concerned, even at this height, it is balanced by production and the only unbalanced term is advection. In fact, the residual term (figs. 5a and 6a) is almost the specular image of advection, which, as results from the [13] measurements, should be balanced by the transport term.

At greater height, in the H8 case (fig. 8a) the model results are in agreement with the measurements within the error band over the entire domain, whereas for V8 (fig. 9a) they are underestimated, expecially over the valley. This different behaviour between the model performances over the two topographies can be explained considering that the destabilizing effect of the concave curvature of the streamlines, still present over the valley and totally absent over the hill [27], induces a perturbation which is poorly described

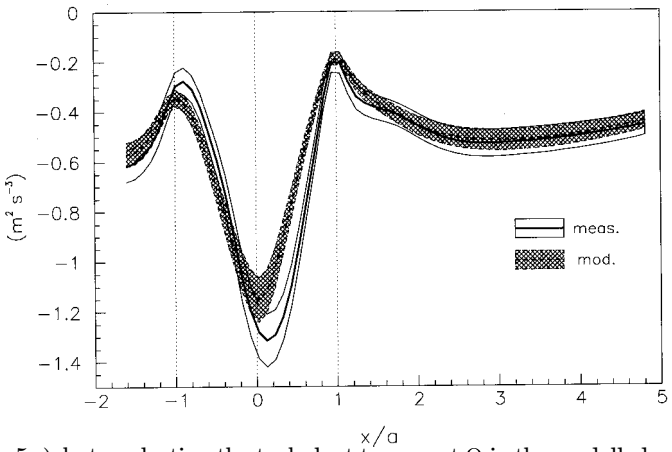

Fig. 7. – As in fig. 5 a), but neglecting the turbulent transport Θ in the modelled part.

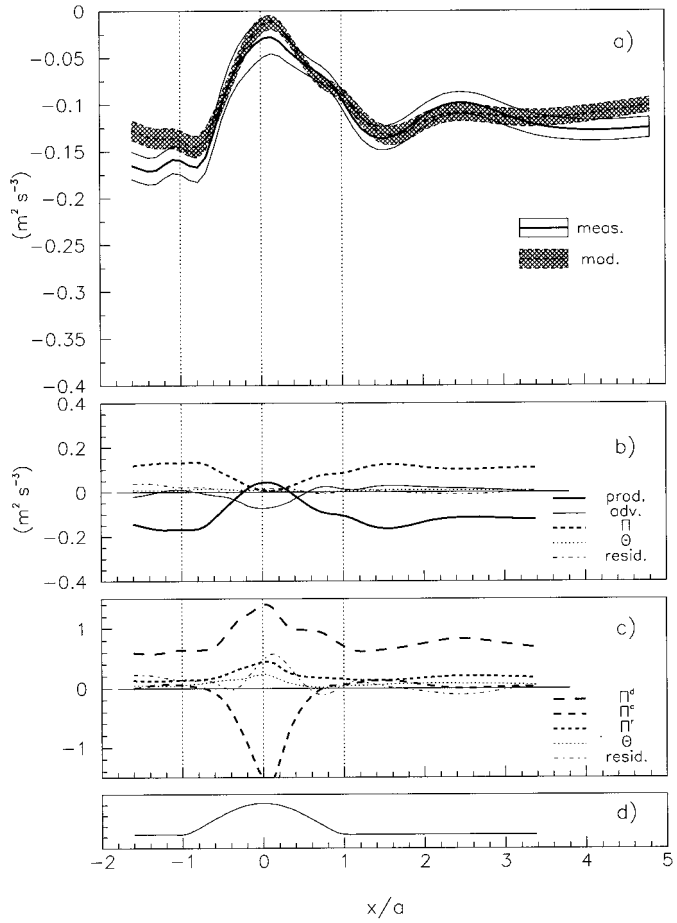

Fig. 8. – As in fig. 1, but for $\hat{z}_{s-\infty} = 2H$ and H8.

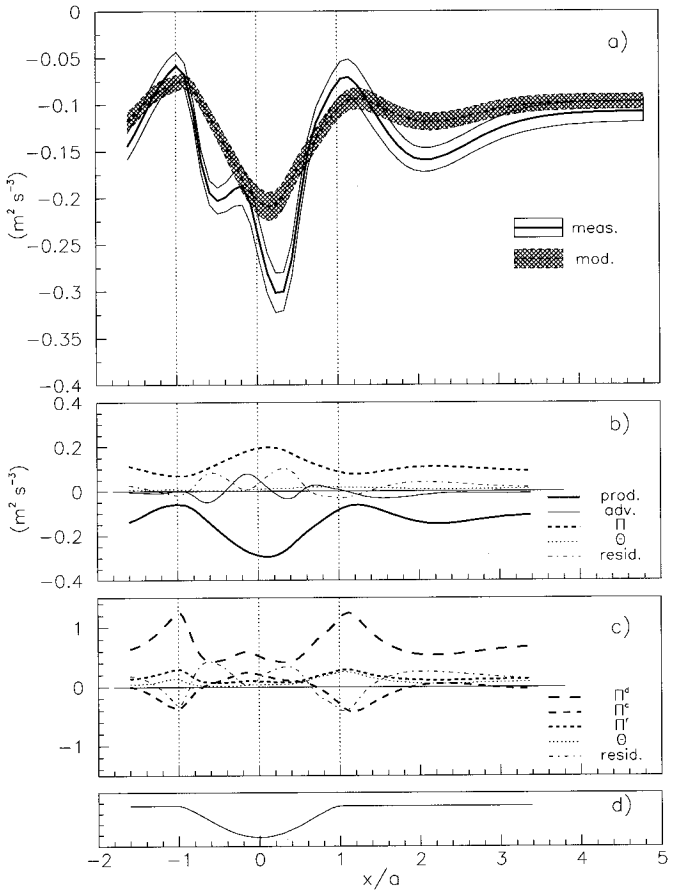

Fig. 9. – As in fig. 8, but for V8.

by models at variance with the stabilizing convex one. The transport term becomes negligible, and the sign of $-\overline{uw^2}$ is correct (except in small zones near $x/a = -0.5$ in V8 and in the lee of H8, see figs. 3 and 4). The residual term for V8 (fig. 9b) takes the same shape (with the opposite sign) as the advection term and, in this case, it seems reasonable to say that the Π^d term does not take the correct form (fig. 9c). In fact, in the present formulation it does not account for the streamwise derivatives which influence advection.

6. – Conclusions

Starting from the profiles of first- and second-order moments of the flow field, measured in a terrain-following coordinate system in a wind tunnel over a gently shaped 2D hill and valley [8, 10], we are able to compute the terms of Reynolds shear stress balance equation in a streamline coordinate system and evaluate their associated errors using a Monte Carlo technique, which takes experimental errors into account. Since the third-order moments are not available, we have modelled the pressure-velocity correlation terms following [6] and the turbulent transport using a flux-gradient diffusion approach for the triple velocity correlation. The comparison between the terms which can be derived directly from the measurements and those modelled in the various regions of

the boundary layer perturbed by the two topographies considered shows that:

i) the flux-gradient assumption gives reliable values (at least the correct sign) of the triple products in the inner layer, where a local equilibrium is present, and in the layer above the streamline originating at about $\hat{z}_{s-\infty} = 2H$. In the intermediate levels, where the perturbations induced by the obstacles are greater and the turbulence dynamics is dominated by the rapid distortion mechanism and curvature effects, large zones of the counter-gradient transport of triple moments are present (prevalently in the lee of the hill or around the end of the valley). In these regions the computed turbulent transport is incorrect and the modelled part is more accurate when this term is ignored.

ii) The prevailing term in the modelled pressure-velocity correlation is everywhere the rapid distortion term which more or less balances the shear production (see [27]). In concave regions the total pressure-strain redistribution may be underestimated and, at higher levels, its rapid distortion part should probably take streamwise advection into account.

A possible parameterization of the triple velocity correlation in the counter-gradient zones, roughly corresponding to the flow regions in which the streamlines show concave curvature, can be made by assuming a proportionality between second- and third-order moments, as occurs in convective conditions [30, 31]. This assumption seems to conform to the analogy between concave streamline curvature and unstable conditions [32].

Furthermore, it has been noted that, because of the difference in horizontal extension of the concave region between V8 and H8 [27], the perturbation induced in V8 has a vertical lenght scale greater than in the H8 case. In fact, quite generally, the perturbation induced in the near-neutral boundary layer by gentle slope topography has a vertical scale roughly comparable to the horizontal one. Then the perturbation induced by the concave curvature region extends, in the V8 case, to greater heights with respect to the convex one. The perturbation produced by the concave curvature is of destabilizing character (see [32]) and turns out to be poorly modelled. This fact justifies the larger volume of fluid where the model does not cope with the observations in the V8 case, with respect the H8 case.

* * *

The authors are indebted to W. H. SNYDER, U. S. EPA, for supplying the data set. This study was partially supported by the EEC Contract CHRX-CT94-0518: "Wind modelling and climatology studies above inhomogeneous terrain with regard to wind energy and air pollution with special emphasis on coastal Mediterranean areas".

REFERENCES

[1] TAYLOR P. A., MASON P. J. and BRADLEY E. F., *Boundary-Layer Meteorol.*, **39** (1987) 107-132.
[2] MASON P. J. and KING J. C., *Q. J. R. Meteorol. Soc.*, **110** (1984) 821-845.
[3] HUNT J. C. R., TAMPIERI F., WENG W. S. and CARRUTHERS D. J., *J. Fluid Mech.*, **227** (1991) 667-688.
[4] YING R., CANUTO V. M. and YPMA R. M., *Boundary-Layer Meteorol.*, **70** (1994) 401-427.
[5] FINARDI S., TROMBETTI F., TAMPIERI F. and BRUSASCA G., *Boundary-Layer Meteorol.*, **73** (1995) 343-356.
[6] ZEMAN O. and JENSEN N. O., *Q. J. R. Meteorol. Soc.*, **113** (1987) 55-80.
[7] MICKLE R. E., COOCK N. J., HOFF A. M., SALMON N. O. J. J. R., TAYLOR P. A., TETZLAFF G. and TEUNISSEN H. W., *Boundary-Layer. Meteorol.*, **43** (1988) 143-169.

[8] KHURSHUDYAN L. H., SNYDER W. H. and NEKRASOV I. V., in *Flow and Dispersion of Pollutants over Two-Dimensional Hills: Summary Report on Joint Soviet-American Study*, EPA-600/4-81-067, Res. Tri. Pk., NC (1981).
[9] GONG W. and IBBETSON A., *Boundary-Layer Meteorol.*, **49** (1989) 113-148.
[10] KHURSHUDYAN L. H., SNYDER W. H., NEKRASOV I. V., LAWSON R. E., THOMPSON R. S. and SCHIERMEIER F. A., *Flow and Dispersion of Pollutants over Two-Dimensional Valleys: Summary Report on Joint Soviet-American Study*, EPA-600/3-90-025, Res. Tri. Pk., NC (1981).
[11] FINNIGAN J. J., RAUPACH M. R., BRADLEY E. F. and ALDIS G. K., *Boundary-Layer Meteorol.*, **50** (1990) 277-317.
[12] BASKARAN V., SMITH A. J. and JOUBERT P. N., *J. Fluid Mech.*, **182** (1987) 47-83.
[13] BASKARAN V., SMITH A. J. and JOUBERT P. N., *J. Fluid Mech.*, **232** (1991) 377-402.
[14] SNYDER W. H., KHURSHUDYAN L. H., NEKRASOV I. V., LAWSON R. E. and THOMPSON R. S., *Atmos. Environ. A*, **25** (1991) 1347-1375.
[15] TROMBETTI F., MARTANO P. and TAMPIERI F., *Data Sets for Studies of Flow and Dispersion in Complex Terrain:* I) *the "RUSHIL" Wind Tunnel Experiment* (*flow data*), Rapporto Tecnico No. 1, FISBAT-RT-91/1 (1991).
[16] BUSUOLI M., TROMBETTI F. and TAMPIERI F., *Data Sets for Studies of Flow and Dispersion in Complex Terrain:* II) *the "RUSVAL" Wind Tunnel Experiment* (*Flow Data*). Technical Paper No. 3, FISBAT-TP-93/1 (1993).
[17] IMSL Math/Library, *FORTRAN Subroutines for Mathematical Applications*, No. MALB-USM-PERFECT-EN8912-1.1. 1989, User Manual, pp. 550-553.
[18] MAURIZI A., DI SABATINO S., TROMBETTI F. and TAMPIERI F., *A method of analysis for turbulent flows using the streamline coordinate system*, *Boundary-Layer Meteorol.*, **82** (1997) 379-397.
[19] FINNIGAN J. J., *J. Fluid Mech.*, **130** (1983) 241-258.
[20] WYNGAARD J. C., *Boundary-layer modeling*, in *Atmospheric Turbulence and Air Pollution Modeling*, edited by F. T. M. NIEUWSTADT and H. VAN DOP (Reidel Publ. Comp., Dordrecht) 1982, pp. 69-106.
[21] TRUESDELL C., *Z. Angew. Math. Mech.*, **33** (1953) 345-356.
[22] ZEMAN O. and TENNEKES H., *J. Atmos. Sci.*, **32** (1975) 1808-1813.
[23] ROTTA J. C., *Z. Phys.*, **129** (1951) 547-572.
[24] HUNT J. C. R., MOIN P., LEE M., MOSER R. D., SPARART P., MANSOUR N. N., KAIMAL J. C. and GAYNOR E., in *Advances in Turbulence 2*, edited by H. H. FERNHOLZ and H. E. FIEDLER (Springer-Verlag, Berlin) 1989, pp. 128-134.
[25] LAUNDER B. E., *Int. J. Heat Fluid Flow*, **10** (1989) 282-300.
[26] DURBIN P. A., *J. Fluid Mech.*, **249** (1993) 465-498.
[27] MAURIZI A., DI SABATINO S. and TROMBETTI F., *Data Sets for Studies of Flow and Dispersion in Complex Terrain:* III) *Turbulence Features in Streamline Coordinates in the "RUSHIL" and "RUSVAL" Wind Tunnel Experiment*, Technical Paper No. 5, FISBAT-TP-95/1 (1995).
[28] JACKSON P. S. and HUNT J. C. R., *Q. J. R. Meteorol. Soc.*, **101** (1975) 929-955.
[29] JENSEN N. O., PETERSEN E. L. and TROEN I., *Extrapolation of Mean Wind Statistics with Special Regard to Wind Energy Application*, World Meteorological Organisation Report WCP-86 (1984).
[30] HUNT J. C. R., KAIMAL J. C. and GAYNOR J. E., *Q. J. R. Meteorol. Soc.*, **114** (1988) 827-858.
[31] LENSCHOW D. H. and STEPHENS P. L., *Boundary-Layer Meteorol.*, **19** (1980) 509-532.
[32] BRADSHAW P., *J. Fluid Mech.*, **36** (1969) 179-191.